Hydrogen-Induced Polymorphism of the Pd(110) Surface

David Tománek,* Steffen Wilke, and Matthias Scheffler
Fritz-Haber Institut der Max-Planck Gesellschaft, Faradayweg 4-6, D-14195 Berlin-Dahlem, Germany
(Received 27 September 1996)

Using density functional theory, we investigate the adsorption of hydrogen on Pd(110). We find this system to be unique in that hydrogen modifies the surface morphology into a multitude of coexisting structures, which are precursors for its solution in the bulk metal. This behavior is manifested in the energetic near degeneracy between the (1×2) paired-row and missing-row structures, and (2×1) structures containing subsurface hydrogen. The uncommon paired-row structure, induced by an incompletely screened Coulomb repulsion between adjacent rows, opens hydrogen diffusion channels into the bulk. [S0031-9007(97)03861-1]

PACS numbers: 82.65.Dp, 68.35.–p, 73.20.At, 82.20.Kh

One traditional focus of interest in surface science has been the "catalytic effect" which a solid surface exhibits to destabilize and break internal bonds of adsorbed molecules [1]. Much less attention has been paid so far to the effect of adsorbates on the atomic geometry of the substrate, which in turn can change profoundly its catalytic behavior. Our theoretical results, presented here, suggest that hydrogen is unique in modifying the morphology of the Pd(110) surface into a rich variety of energetically near-degenerate structures. The associated polymorphism is expected to result in structural changes at catalytically active sites during reactions. Detailed information about the equilibrium adsorption geometry also sheds further light on the likely mechanism of hydrogen entering into bulk metals.

Whereas the clean (110) surfaces of the late $5d$ metals Ir, Pt, and Au reconstruct spontaneously [2–5], it takes a high coverage of hydrogen to induce reconstruction on the (110) surface of the late $4d$ metal Pd [6–11]. With increasing hydrogen coverage, the low energy electron diffraction (LEED) pattern of the Pd(110) surface has been observed to change from a (1×1) to a (2×1) and finally a (1×2) superstructure at low surface temperatures $T_s \lesssim 200$ K [12,13]. Experimental data suggest that the (2×1) superstructure at one monolayer (ML) coverage arises from an ordered hydrogen superlattice on an unreconstructed Pd surface [14,15], and that the (1×2) structure involves a reconstruction of the substrate [7–11]. Whereas several observations [8,11,16] seem to favor the paired-row model for H/Pd(110)-(1×2), both the missing-row [17] and the paired-row [18] models of reconstruction have been discussed for the hydrogen-covered Ni(110)-(1×2) surface which shows a very similar behavior. Beyond this rich variety of structures, many other surface geometries have been observed on Pd(110) when the system was heated [7–9,11].

The large number of partly conflicting experimental results calls not only for a bias-free determination of the atomic geometry, but even more for the explanation of the physical origin of hydrogen-induced surface reconstruction. In the following, we will argue that the H/Pd(110) system is unique in that many vastly different geometrical arrangements are energetically near degenerate. Even large-scale atomic rearrangements may occur rapidly in the presence of the highly diffusive hydrogen, leading to a further enhancement of polymorphism [7,19]. The resulting coexistence of different structures would explain apparent controversies between experimental data.

In the following, we will describe the likely coexisting equilibrium structures and identify the driving forces for structural transitions on the clean and hydrogen-covered Pd(110) surface using *ab initio* calculations. We will discuss the energetics of structural transitions in terms of the changing surface energy E_s *per surface Pd atom.* For a sufficiently thick N-layer metal slab, this quantity is given by [20]

$$E_s^0 = \tfrac{1}{2}\,(E_{\text{Pd-slab}}^{\text{total}} - N E_{\text{Pd-bulk}}^{\text{total}}) \tag{1}$$

for the clean surface and

$$E_s(\Theta) = \tfrac{1}{2}\,(E_{\text{H/Pd-slab}}^{\text{total}} - N E_{\text{Pd-bulk}}^{\text{total}}) - \Theta(E_{\text{H-atom}}^{\text{total}} + \tfrac{1}{2} E_{\text{H}_2}^{\text{dis}}) \tag{2}$$

for the hydrogen-covered surface. The total energies for Pd systems are given per Wigner-Seitz cell, containing one atom in the bulk and N atoms in the slab. Θ denotes the hydrogen coverage, and the factor $1/2$ accounts for the two (identical) surfaces of the slabs.

We used two different implementations of the density functional theory (DFT) [21] to calculate the equilibrium structures and the total energies E^{total} of clean and adsorbate-covered surfaces [22]. For geometry optimization, we used the full-potential linear augmented-plane wave method (FP-LAPW) [23,24] that yields metastable and stable geometries via a damped molecular-dynamics approach. Nonlocal terms in the exchange-correlation functional were described using the generalized gradient approximation (GGA) [25] that had been used to describe hydrogen adsorption on Mo(110) [26] and Pd(100) [27]. For the sake of comparison, we calculated surface energies also using the *ab initio* pseudopotential method

with a local orbital basis [28], based on the local density approximation (LDA) [29] for the exchange-correlation functional. This method had been used to describe the interaction of hydrogen with different Pd surfaces [20,30] and with bulk Pd [31].

We modeled the metal surface by a periodic arrangement of seven-layer slabs [32] with a (110) surface, separated by 10 Å thick vacuum regions. Hydrogen atoms were adsorbed on both sides of the slab when describing covered surfaces. All hydrogen atoms and all atoms in the topmost two Pd layers were allowed to relax on top of a rigid "bulk" structure. The basis and further computational details have been outlined in Ref. [27] for the full-potential GGA calculation, and in Refs. [20,30,31] for the pseudopotential LDA calculation. All calculations have been performed nonrelativistically. Results obtained by the two computational techniques for the key quantity of interest, namely, surface energy differences ΔE_s, were found to agree to better than 0.05 eV.

Our calculations indicate that for the clean Pd(110)-(1×1) surface, the topmost interlayer spacing contracts with respect to the bulk value d_0 by $\Delta d_{12}/d_0 = -8.2\%$, whereas the distance between the second and third layers expands by $\Delta d_{23}/d_0 = +0.7\%$. These values are in good agreement with the observed LEED data of Ref. [14], $\Delta d_{12}/d_0 = (-5.1 \pm 1.5)\%$, $\Delta d_{23}/d_0 = (+2.9 \pm 1.5)\%$, and $\Delta d_{12}/d_0 = (-5.7 \pm 2)\%$, $\Delta d_{23}/d_0 = (+0.5 \pm 2)\%$ of Ref. [33]. Our LDA value $E_s^0 = 1.27$ eV for the surface energy of clean Pd(110)-(1×1) lies somewhat higher than the GGA value $E_s^0 = 1.1$ eV, confirming the trend that LDA-based surface energies lie generally 0.2 eV above GGA-based values. We find the surface energy value for the unreconstructed system to be only 0.02 eV lower than that of a missing-row reconstructed surface, indicating a tendency towards multiple metastability of even the clean surface. The calculated work function of the clean Pd(110) surface, based on GGA, is $\phi_{\mathrm{GGA}} = 4.85$ eV.

Our results for the Pd(110) surface at $\Theta = 1.0$ ML coverage suggest that hydrogen atoms adsorb preferably in highly coordinated surface sites [6,27], such as the quasithreefold (QT) coordinated sites and the long-bridge (LB) adsorption sites. We found that in both cases hydrogen atoms seek threefold coordination and form a (2×1) "zigzag" superstructure. Even though no reconstruction is induced at this coverage, the substrate geometry is modified significantly. The calculated interlayer spacing changes $\Delta d_{12}/d_0 = -3.2\%$, $\Delta d_{23}/d_0 = +1.4\%$, and the Pd-H distance $d_{\mathrm{H-Pd}} = 1.8$ Å compares favorably with the LEED data of Ref. [14], $\Delta d_{12}/d_0 = (-2.2 \pm 1.5)\%$, $\Delta d_{23}/d_0 = (+2.9 \pm 1.5)\%$, and $d_{\mathrm{H-Pd}} = 2.0 \pm 0.1$ Å.

We find that the presence of one monolayer hydrogen reduces the surface energy of Pd(110) to $E_s(\Theta = 1) = 0.95$ eV within the LDA. The small surface energy difference between the QT and the LB adsorption geometry of only $\Delta E_s(\Theta = 1) = 0.02$ eV suggests a coexistence of various hydrogen arrangements even at low temperatures. The work function, which shows a stronger dependence on the surface morphology than the surface energy, should be more useful to identify surface structures. We find that at $\Theta = 1$ ML coverage the work function of these structures increases by $\Delta\phi_{\mathrm{GGA}}(\mathrm{QT}) = +0.15$ eV and $\Delta\phi_{\mathrm{GGA}}(\mathrm{LB}) = +0.07$ eV with respect to the clean surface. Comparison between these and the observed values $\Delta\phi_{\mathrm{expt}} = +0.22$ eV [34] and $\Delta\phi_{\mathrm{expt}} = +0.24$ eV [15], together with the slight energetic preference for the QT adsorption geometry, suggests the QT structure to prevail.

At the higher coverage $\Theta = 1.5$, hydrogen appears to affect the substrate geometry even more significantly. We focus our calculations on the paired-row (PR) and missing-row (MR) geometries, the favorite structural candidates for the (1×2) reconstructed surface [8,11,16–18], and compare our results to the unreconstructed (2×1) phase containing hydrogen atoms in subsurface sites (SS) [see Fig. 1(a)]. We generated the paired-row reconstructed surface by placing 1.0 ML of hydrogen in quasithreefold coordinated trough sites and the remaining 0.5 ML of hydrogen in either long-bridge sites or on top of second-layer Pd atoms in the troughs. To obtain the unreconstructed Pd(110) phase with subsurface hydrogen, we placed 1.0 ML of hydrogen in the trough sites and 0.5 ML of hydrogen in octahedral subsurface sites. The missing-row surface was constructed by placing 1.0 ML of hydrogen in quasithreefold coordinated sites between the two topmost Pd layers and the remaining 0.5 ML of hydrogen in the QT and LB trough sites. The optimized surface geometries and surface energy differences for the PR, MR, and SS structures are presented in Fig. 1.

Calculated surface energy differences between the different substrate structures and adsorption geometries for $\Theta = 1.5$ ML were all found to be very small, of the order $\Delta E_s \lesssim 0.06$ eV. This result suggests that no single

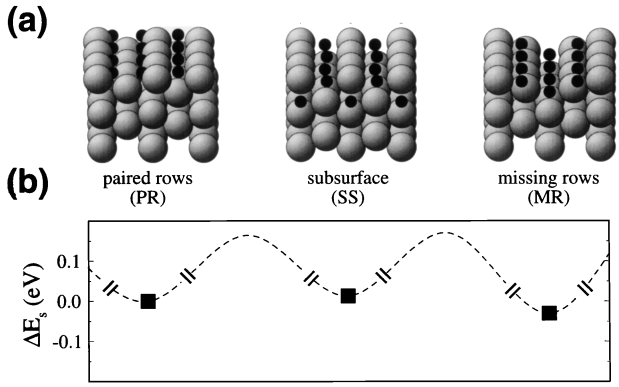

FIG. 1. (a) Schematic view of the Pd(110)-(1×2) paired-row reconstructed surface (PR), the Pd(110)-(2×1) reconstructed surface with occupied subsurface sites (SS), and the Pd(110)-(1×2) missing-row reconstructed surface (MR), all at hydrogen coverage $\Theta = 1.5$. (b) Density functional results for the surface energy differences ΔE_s of these structures with respect to the Pd(110)-(1×2) paired-row structure (■). The dashed line connecting these data points indicates a nonzero activation barrier between these structures.

structure is energetically preferred, but rather that many different phases should coexist even at room temperature. Still, transition between these structures may be hindered by energy barriers, indicated schematically in Fig. 1(b). In this likely case, the actual surface structure may depend crucially on the preparation conditions, which could partly explain apparent inconsistencies in the experimental data. In view of this fact and the sensitivity of the work function on the substrate and adsorbate structure, we do not expect perfect agreement between the calculated and observed work function values for any of our structures. Indeed, the calculated values span a wide range from $\Delta\phi_{\mathrm{GGA}} = -0.120$ eV for the subsurface structure to $\Delta\phi_{\mathrm{GGA}} = +0.380$ eV for the missing-row structure with respect to the clean surface, depending sensitively on the adsorption geometry. The work function values observed at the (1×2) surface, $\Delta\phi_{\mathrm{expt}} = +0.300$ eV [34] and $\Delta\phi_{\mathrm{expt}} = +0.325$ eV [15], fall into the range of calculated values, and are most consistent with our results for the paired-row and the missing-row surfaces.

The high stability of the missing-row structure comes as no surprise, since this is the favored reconstruction pattern of (110) surfaces of late $5d$ metals [2–5]. Much more interesting is the reason for the stability of the paired-row reconstructed surface, shown schematically in Fig. 2(b). We label the horizontal displacement of the topmost rows by δx and note the energetic degeneracy of the isomorphic structures with $+\delta x$ and $-\delta x$. This atomic geometry is also interesting from the point of view of opening hydrogen diffusion channels into the bulk. Our results for the energetics of the Pd(110)-(1×2) paired-row reconstruction at the hydrogen coverages $\Theta = 0.0, 1.0, 1.5$ are summarized in Fig. 2.

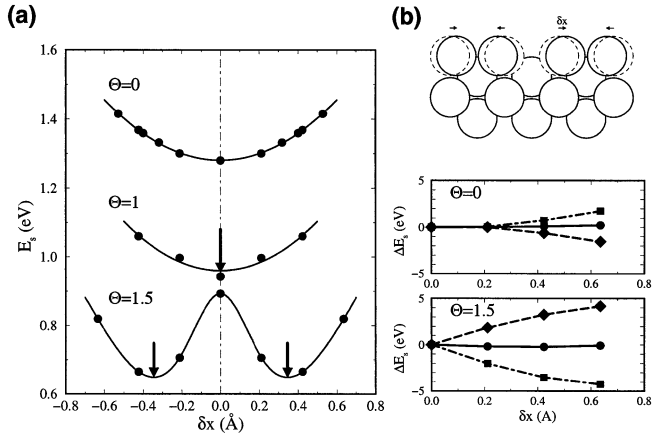

FIG. 2. (a) Surface energy of clean and hydrogen-covered ($\Theta = 1.0, 1.5$) Pd(110) surfaces as a function of the row-pairing relaxation δx of Pd atoms in the topmost layer. (b) Schematic side view of a paired-row reconstructed surface, showing the quantity δx. Also shown is the change of the surface energy ΔE_s due to row pairing (• and solid line) for a clean ($\Theta = 0$) and a H-covered ($\Theta = 1.5$) Pd(110) surface. The trend is given by the band structure contribution to ΔE_s (■ and dash-dotted line) and counteracted by the Coulomb term (◆ and dashed line).

As shown in Fig. 2(a), the surface energy of a clean surface is minimized in the unreconstructed geometry, given by $\delta x = 0$. One monolayer coverage of hydrogen not only lowers the surface energy, but also reduces the energy cost of row pairing. Even at this higher coverage, there is no energetic gain upon row pairing. Increasing the hydrogen coverage to $\Theta = 1.5$ lowers the surface energy further, but is accompanied by a decrease of the site-averaged hydrogen adsorption energy by ≈ 0.1 eV due to a significant repulsion in the hydrogen adlayer. To reduce this repulsion, the system responds by pairing the Pd rows, resulting in an energy gain of 0.22 eV per surface atom. The predicted row displacement $\delta x = 0.32$ Å and the large vertical buckling of second-layer Pd $\delta z(\mathrm{Pd}) = 0.3$ Å for the paired-row reconstructed surface [see Figs. 1(a) and 2(b) for a schematic view] are in very good agreement with the observed values $\delta x_{\mathrm{expt}} = 0.2$–$0.4$ Å and $\delta z_{\mathrm{expt}}(\mathrm{Pd}) = 0.3$–$0.44$ Å [8,9].

While this calculation establishes the paired-row structure as a good candidate for a hydrogen-covered surface, the total energy itself says little about the driving force for row pairing. In order to understand the mechanism of this reconstruction, we subdivided the total energy into band structure energy, given by the contribution of the occupied states to the first moment of the density of states, and a second term which is dominated by the Coulomb energy. The contribution of these two terms to the surface energy differences upon row pairing is shown in Fig. 2(b). We found that at zero and 1.0 ML coverage, the band structure contribution to the surface energy favors row pairing, whereas for $\Theta = 1.5$ this term *disfavors* row pairing. Since this behavior is just opposite the trend in the total energy, we can exclude the Peierls instability as a source of this type of reconstruction. In contrast to the band structure term, the Coulomb energy contribution to surface energy differences always shows in the same direction as the total energy itself. This leads us to conclude that the paired-row reconstruction is driven by a gain in Coulomb energy.

The onset of reconstruction only at high hydrogen coverages suggests an intimate link between changes in the Coulomb energy and the charge distribution near the adsorbed hydrogen atoms. In Fig. 3 we present the difference charge density on the unreconstructed Pd(110) surface at $\Theta = 1.0$ and the (1×2) reconstructed surface at $\Theta = 1.5$. Independent of coverage, we find that hydrogen atoms accumulate an excess charge of 0.1–$0.2e$ upon adsorption on Pd(110). This is also true in those trough sites on the Pd(110) surface that contain two hydrogen atoms [left panel in Fig. 1(a) and lower half of Fig. 3(b)]. The lack of screening charge in the middle of the troughs, indicated by a horizontal "band" of low screening charge density in the lower half of Fig. 3(b), leads to a net gain in the Coulomb energy when these hydrogen atoms increase their mutual distance, by pushing the corresponding neighboring rows apart.

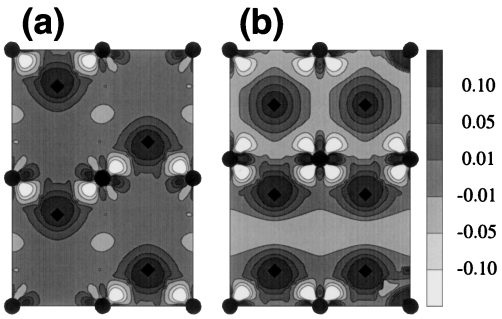

FIG. 3. Charge density difference Δn (with respect to a superposition of atomic charge densities) for (a) the unreconstructed Pd(110) surface, covered by an ordered monolayer of hydrogen, and (b) the Pd(110)-(1×2) paired-row reconstructed surface with $\Theta = 1.5$ hydrogen coverage. The contour plot of Δn is shown in the plane of the hydrogen atoms. The position of Pd atoms is indicated by (●), that of H atoms by (◆).

The likely scenario of hydrogen adsorption on Pd(110) and its solution in the bulk appears to be the following. At coverages up to $\Theta = 1.0$, hydrogen atoms preferentially occupy the quasithreefold coordinated trough sites. A further increase of the coverage leads to the troughs becoming filled with a dense hydrogen phase. To counteract their mutual, incompletely screened Coulomb repulsion, hydrogen atoms push locally the neighboring surface rows apart, thereby opening channels to subsurface sites which can accommodate such atoms at little cost to the surface energy [see Fig. 1(b)]. Consequently, we expect a coexistence between the paired-row and the subsurface structures. A concerted exchange mechanism, on the other hand, may assist in the formation of the missing-row structure that requires large mass transport.

The low energy differences between various morphologies in a surface region saturated by hydrogen will likely lead to the coexistence of more than the three structures discussed here. Owing to the sensitive dependence of the work function on the surface morphology, we suggest to obtain more detailed information about the successive steps occurring during the adsorption of hydrogen on Pd(110) by careful measurements of the work function as a function of hydrogen coverage.

We would like to thank Klaus Christmann and Jürgen Behm for fruitful discussions, and Zhijun Sun for assistance with the pseudopotential calculations. One of us (D. T.) acknowledges the hospitality of the Theory Group at the Fritz-Haber Institut in Berlin and partial financial support by the Office of Naval Research under Grant No. N00014-90-J-1396.

*Permanent address: Department of Physics and Astronomy, Michigan State University, East Lansing, Michigan 48824–1116.

[1] *The Chemical Physics of Solid Surfaces and Heterogeneous Catalysis*, edited by D. A. King and D. P. Woodruff (Elsevier, Amsterdam, 1982), Vol. 4.
[2] W. Moritz and D. Wolf, Surf. Sci. **163**, L655 (1985).
[3] C. M. Chan and M. A. van Hove, Surf. Sci. **171**, 226 (1986).
[4] M. Copel and T. Gustafsson, Phys. Rev. Lett. **57**, 723 (1986).
[5] P. Fery, W. Moritz, and D. Wolf, Phys. Rev. B **38**, 7275 (1988).
[6] K. Christmann, Mol. Phys. **66**, 1 (1989).
[7] J. Yoshinobu, Hiroyuki Tanaka, and Maki Kawai, Phys. Rev. B **51**, 4529 (1995).
[8] H. Niehus, C. Hiller, and G. Comsa, Surf. Sci. **173**, L599 (1986).
[9] G. Kleinle *et al.*, Surf. Sci. **189**, 177 (1987).
[10] E. Kampshoff *et al.*, Surf. Sci. **360**, 55 (1996).
[11] K. H. Rieder, M. Baumberger, and W. Stocker, Phys. Rev. Lett. **51**, 1799 (1983).
[12] K. Christmann *et al.*, Solid State Commun. **51**, 487 (1984).
[13] R. J. Behm *et al.*, J. Chem. Phys. **78**, 7486 (1983).
[14] M. Skottke *et al.*, J. Chem. Phys. **87**, 6191 (1987).
[15] M.-G. Cattania *et al.*, Surf. Sci. **126**, 382 (1983).
[16] M. Baumberger, W. Stocker, and K. H. Rieder, Appl. Phys. A **41**, 151 (1986).
[17] J. R. Jones *et al.*, Surf. Sci. **147**, 1 (1984).
[18] J. E. Demuth, J. Colloid Interface Sci. **58**, 187 (1977).
[19] The bulk counterpart of this behavior is the hydrogen enhanced local plasticity (HELP) mechanism of "hydrogen embrittlement," described in C. D. Beachem, *Hydrogen Damage* (American Society for Metals, Metals Park, OH, 1977).
[20] D. Tománek, Z. Sun, and S. G. Louie, Phys. Rev. B **43**, 4699 (1991).
[21] P. Hohenberg and W. Kohn, Phys. Rev. **136**, B864 (1964).
[22] We eliminate systematic errors in the surface energy at nonzero hydrogen coverage by using $E_{\mathrm{H-atom}}^{\mathrm{total}} = 13.60$ eV for the total energy of the H atom and the experimental value $E_{\mathrm{H_2}}^{\mathrm{dis}} = 4.75$ eV for the dissociation energy of the H_2 molecule instead of the less accurate density functional values in Eq. (2).
[23] P. Blaha, K. Schwarz, and R. Augustyn, WIEN93, Technical University of Vienna, 1993.
[24] Our force calculation follows the description of R. Yu, D. Singh, and H. Krakauer, Phys. Rev. B **43**, 6411 (1991). Further details are given in B. Kohler *et al.*, Comput. Phys. Commun. **94**, 31 (1996).
[25] J. P. Perdew *et al.*, Phys. Rev. B **46**, 6671 (1992).
[26] B. Kohler *et al.*, Phys. Rev. Lett. **74**, 1387 (1995).
[27] S. Wilke and M. Scheffler, Phys. Rev. B **53**, 4926 (1996); Surf. Sci. **329**, L605 (1995).
[28] C. T. Chan, David Vanderbilt, and Steven G. Louie, Phys. Rev. B **33**, 2455 (1986); C. T. Chan *et al.*, Phys. Rev. B **33**, 7941 (1986).
[29] W. Kohn and L. J. Sham, Phys. Rev. **140**, A1133 (1965).
[30] D. Tománek, S. G. Louie, and C. T. Chan, Phys. Rev. Lett. **57**, 2594 (1986); **58**, 287(E) (1987).
[31] Z. Sun and D. Tománek, Phys. Rev. Lett. **63**, 59 (1989).
[32] A slab of this thickness represents the surface adequately, since the surface energy differs from a five-layer slab by merely 0.05 eV.
[33] R. D. Diehl *et al.*, J. Phys. C **18**, 4069 (1985).
[34] J.-W. He *et al.*, Surf. Sci. **198**, 413 (1988).